The adsorption of the orange acid dye 52 in aqueous solutions by the biochar of the seeds and shells of Cistus Ladaniferus

H. El Farissi[1], R. Lakhmiri[1*], A. Albourine[2] and M. Safi[3]

Abstract— The presence of dyes in aquatic systems has become a serious problem. As a result, much attention has been paid to new technologies for the removal of dyes from contaminated waters. Biosorption is one of those emerging technologies that use natural waste to sequester dyes from industrial wastewater. In this study, we realized the kinetics of elimination of orange acid 52 in solution by adsorption on bio-char seeds and shells of Cistus ladaniferus((BCCLS and BCCLSh). The BCCLS and BCCLSh are biomaterials used as bio-adsorbents for the removal of orange acid 52. The adsorption kinetics of the dye by BCCLS and BCCLSh are correctly described by the pseudo-second order model with a high correlation coefficient (R^2=0.998 for BCCLS and R^2=0.999 for BCCLSh). From the four models adsorption isotherm tested, Langmuir is the appropriate model for both adsorbents. The very high adsorption capacity reaches a value of 500mg.g^{-1} for the BCCLSh and 358.48mg.g^{-1} for the BCCLS.

Index Terms- Cistus ladaniferus - Orange acid 52- Anionic dye - Bio-char - Pyrolysis.

1. INTRODUCTION

Wastewater from industrial sludge in textile mills is generally rich in dyes and organic matter. The elimination of these dyes has received a lot of attention in recent years, not only because of its potential toxicity but also because of its visibility problems. Recent studies indicate that about 13% of the synthetic textile dyes used each year are lost during manufacturing and processing operations and that 22% of these dyes are introduced into the environment by effluents from industrial waste treatment [1]. From an environmental point of view, the elimination of synthetic dyes is very worrying. Among many chemicals and physical methods, sorption has evolved to become one of the most effective processes for discoloration of textile wastewater.

- *H. El Farissi, Laboratory of Chemical Engineering and Valorization of the Resources, Faculty of Sciences and Techniques of Tangier, Abdelmalek Essaâdi University, Km 10 route de Ziaten, BP 416 Tangier, Morocco.*
- *R. Lakhmiri, Laboratory of Chemical Engineering and Valorization of the Resources, Faculty of Sciences and Techniques of Tangier, Abdelmalek Essaâdi University, Km 10 route de Ziaten, BP 416 Tangier, Morocco. PH- +212661427257 lakhmirir@yahho.fr*
- *A. Albourine, Laboratory of Materials and Environment, Team of Coordination Chemistry, Faculty of Sciences, Ibn Zohr University, BP 8106, 80000 Agadir, Morocco.*
- *M. Safi, Laboratory of Physical Chemistry and Bio-Organic Chemistry, URAC University of Hassan II Mohammedia- Casablanca, Faculty of Sciences and Techniques-Mohammedia, BP 146,Mohammedia, Morocco.*

Activated carbon is the most widely used adsorbent, due to its adsorption capacity, higher specific surface area and different pores. Currently, there is increasing interest in the use of inexpensive and unconventional alternative materials in place of traditional adsorbents. Several researchers are studying the use of alternative materials which, although less efficient, involve lower costs. We have Studied the removal of the reactive dye RR-23 by the biochar of the cistus seeds [2]. Thus the elimination of the same dyes by other biomass such as chitosan [3, 4] and silica-chitosan composite in single and binary systems [5].

The objective of this research is to determine the feasibility of using the biochar of cistus ladaniferus seeds (BCCLS) and biochar of cistus ladaniferus shells (BCCLSh) for the removal of anionic dyes orange acid 52 (AO-23).

2. MATERIAL AND METHODS

2.1. The adsorbent

The BCCLS and BCCLSh are two materials used for the removal of AO-52 dye; The BCCLS and BCCLSh are produced by pyrolysis [6,7] obtained in optimal conditions, a temperature equal to 450°C, a particle size of 0.3 to 0.6 mm and a heating rate equal to 21°Cmin^{-1} for the BCCLS and a particle size of 2 to 3 mm and a heating rate of 40°Cmin^{-1} for the BCCLSh. The biochar is then milled in a ceramic mill until the particle sizes are between 0.1 and 0.2 mm.

2.2. Characterization of the cistus seeds and the bio-char

Characterization of the BCCLSs and their BCCLSh obtained under the optimal conditions of pyrolysis were characterized by X-ray fluorescence (Table 1), SEM scanning electron microscope (Figures 1, 2 and 3) and Fourier transform infrared (FTIR) results are shown below (Figure 4 and 5):

TABLE 1

CHEMICAL X-RAY FLUORESCENCE ANALYSIS OF BCCLS AND BCCLSH (CONTENT EXPRESSED AS% CONCENTRATION)

Name of Compound	Weight %	
	Bio-char of Cistus Ladaniferus Shell (BCCLSh)	Bio-Char of Cistus Ladaniferus Seed (BCCLS)
C	71.7	71.5
O	26.7	26.4
K	0.704	0.945
P	0.0423	0.402
Ca	0.383	0.309
Mg	0.0248	0.111
Na	0.0211	****
Fe	0.04	0.0114
Cl	0.175	0.0732
Si	0.0633	0.0217
S	****	0.162
Mn	0.0157	0.0238
Al	0.0167	0.00565
Zn	0.0112	0.00908
Cu	0.0105	0.00642
I	0.0071	0.00604

SEM analysis allows microscopic characterization of the BCCLS and BCCLSh contact surface by means of an SH-4000M apparatus. (Figure 1) shows the results obtained by SEM on particles (0.1 - 0.2 mm in size) of BCCLS and the (figure 2) shows the results SEM of BCCLSh.

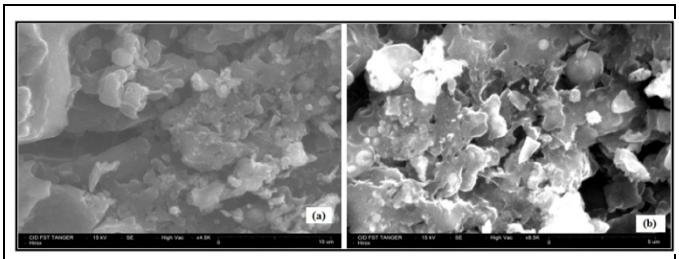

Fig. 1. Micrographs (G * 4500) (a) and (G * 8500) (b) of the BCCLS

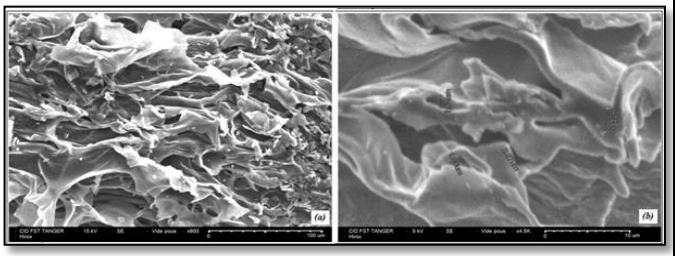

Fig. 2. Micrographs (15kv, G*600)(a) and (5kv, G*4500)(b) of BCCLSh

The EDXA spectrum of BCCLS (a) and the BCCLSh (b) (Figure 3) also confirms the presence of a high percentage of carbon and oxygen in the two materials in addition to the presence of other elements such as K, P, Mg, Ca and Si in BCCLS. The micrographic image of BCCLS and BCCLSh are shown in (figure 1 and 2) respectively, which giving a clear idea on the morphology of materials by the presence of micro-pores and nano-pores which favors the adsorption of AO-52 on the two materials.

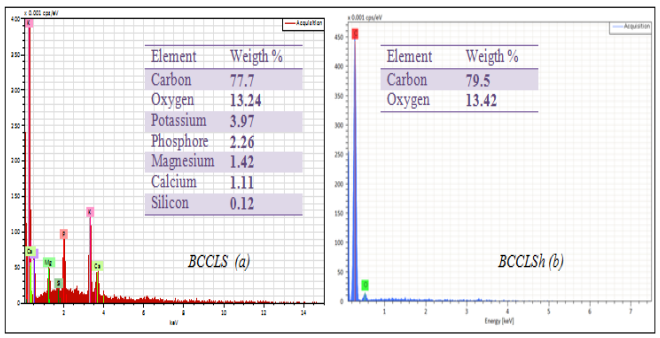

Fig. 3. EDXA spectra of BCCLS (a) and BCCLSh (b)

Fourier transform infrared spectroscopy (FTIR) reveals the chemical groups present in the BCCLS and BCCLSh (Figure 4 and 5)

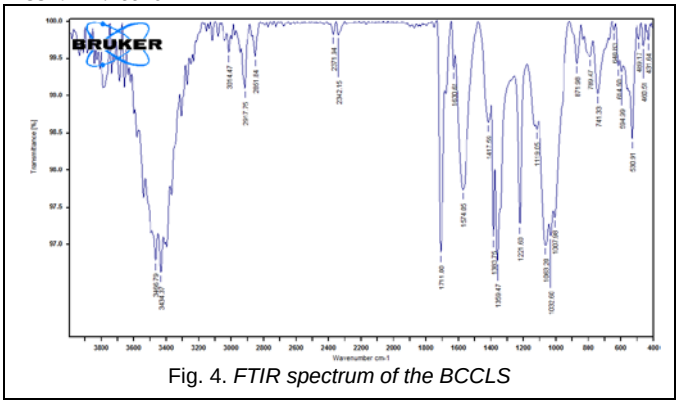

Fig. 4. *FTIR spectrum of the BCCLS*

The BCCLS analysis by TFIR (Figure 4) showed N-H bonds of amines in symmetric and antisymmetric vibration between 3410 - 3500cm^{-1} and C-H bonds of vinyl and alkanes between 3010-3040cm^{-1} And 2850-2925cm^{-1} respectively, phosphines between 2280-2410cm^{-1}, C=O of aromatic ketones, amides and carboxylic acids between 1650-1725cm^{-1}, 1630-1710cm^{-1} and 1400-1450Cm^{-1} respectively. The C-O bonds of the primary and secondary alcools between 1050-1080cm^{-1} and between 1085-1125cm^{-1}, C-O bonds of ether between 1000-1050cm^{-1}, aromatics between 730-890cm^{-1} and finally the presence of the cycloalkane and nitriles between 530-580cm^{-1} and 430-480cm^{-1}.

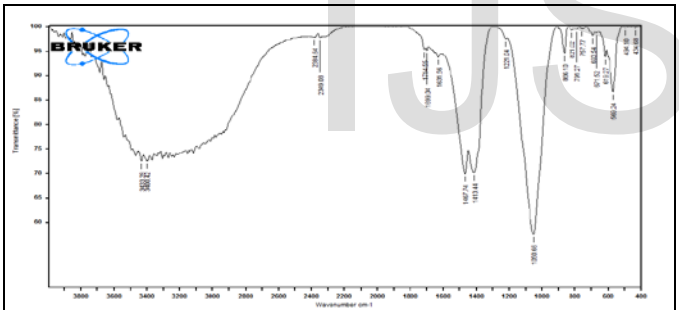

Figure 5: FTIR spectrum of the BCCLSh

The FTIR spectrum in figure 5, of BCCLSh shows the presence of -OH groups of the first and secondary alcohols and phenols between 3000 to 3650 cm^{-1}. This is confirmed by the presence of the antisymmetric vibrations of the -CH_2 to 2925cm^{-1}, -OH bonds free at 3670cm^{-1}. The presence of phosphines with poor peaks between 2280 to 2410cm^{-1}, C=O esters (lactams at four centers) between 1720 to1765 cm^{-1}, aromatic amines at 1515 cm^{-1}, isopropyl group $(CH_3)_2CH$- bonds between 990 to 1050 cm^{-1}, C-N bonds of the nitrile derivatives at 834 cm^{-1}, Ar-OH bonds at 602 cm^{-1}, nitriles between 530 to 580 cm^{-1}, C-C-C-N bonds of the cyclanes between 430 to 580cm^{-1}.

2.3. Adsorbate AO-52

The dye used in this study is the acid orange 52 (AO-52), is an anionic dye, the dye stock solution was prepared by dissolving 0.4 g of AO-52 in 1L of distilled water and the required concentration of the working dye solution was prepared by diluting the stock solution with water distilled.

TABLE 2
PHYSICOCHEMICAL CHARACTERISTICS OF THE AO-52 DYE

Usual name	Acid Orange 52 (AO-52)
Chemical formula	$C_{14}H_{14}N_3S\,O_3Na$
Molecular weight	327.334 g.mol^{-1}
Solubility in water	High
λ_{max} (nm)	464

2.4 Adsorption Process

2.4.1Adsorption kinetics.

The adsorption kinetics are studied only on the BCCLS and BCCLSh, operating under optimum conditions (PH = 7 ± 0.5, adsorbent dose [0.1- 0.2 mm] = 50 mg, dye concentration 300mg.L^{-1}, stirring speed = 200tr.min^{-1} in Erlenmeyer rode 50 mg of the adsorbent are mixed with 50 ml of the AO-52 solution (C_0=300mg.L^{-1}). The suspension is stirred at 200tr.min^{-1} at room temperature (30 ± 1°C). At defined time intervals ranging from 10 to 120 min, the BCCLS and BCCLSh are separated from the liquid by centrifugation. The concentration of the AO-52 in the liquid phase is then determined by measuring the absorbance at 464 nm and reading on a calibration curve established from a range of AO-52 concentrations ranging from 0.0 to 400mg.L^{-1}. The amount of AO-52 (Q_t) adsorbed by two materials as a function of time are calculated according to the following formula (eq.1).

$$Q_e = \frac{(C_0 - C_e)*V}{m} \quad \text{(eq.1)} \qquad R\% = \frac{(C_0 - C_e)}{C_0} * 100 \quad \text{(eq.2)}$$

C_0: concentration initial dye in (mg.L^{-1}); C_e: final dye concentration in solution (mg.L^{-1}); V: volume of the dye solution in L; m: mass of BCCLS or BCCLSh in g; R%: Removal; Q_e: Amount adsorbed in (mg.g^{-1})

The four linear models tested for adsorption kinetics of AO-52 dye by BCCLS and BCCLSh are shown in table 3.

TABLE 3
THE FOUR LINEAR MODELS OF KINETICS

Models	Plotting	Linear Equation
Pseudo-1st-order	$Ln(Q_e-Q_t)$ =f(t)	$Ln(Q_e - Q_t) = -K_1 t + Ln Q_e$ [8,9]
Pseudo-2nd-order	$\frac{t}{Q_t}$ = f(t)	$\frac{t}{Q_t} = \frac{t}{Q_e} + \frac{1}{K_2 Q_e^2}$ [10,11]
Elovich model	Q_t = f(Ln(t))	$Q_e = \frac{1}{\beta} Ln\, t + \frac{1}{\beta} Ln\,(\alpha\beta)$ [12]
Intraparticule diffusion model	$Q_t = f(\sqrt{t})$	$Q_e = K_i \sqrt{t} + C$ [13]

Where q_e: the dye amount adsorbed at equilibrium (mg.g^{-1}), q_t: the dye amount adsorbed at time t (mg.g^{-1}), K_1 is the adsorption rate constant (mL.min^{-1}), t: contact time (min), K_2 (g.mg^{-1}.min), α is the initial adsorption capacity (mg.g^{-1}.min), β is the desorption constant (g.mg^{-1}), K_i is the intraparticule diffusion rate constant. The value of the ordinate at the origin C provides an indication of the thickness of the boundary layer.

2.4.3 Obtaining and modeling of the adsorption isotherm.

To obtain the adsorption isotherm, a series of Erlenmeyer is used. In each Erlenmeyer are poured 50 ml of AO-52 solution dye of varying concentrations: 0; 50; 100; 150; 200; 250; 300; 350; 400; 450 and 500 mg.L^{-1}. The adsorption equilibrium study is carried out under the same optimum conditions indicated above. After equilibration, the particles of the adsorbent are separated by centrifugation and the clarified solution is analyzed by determination of the equilibrium concentration (C_e) of AO-52 using the same calibration curve used previously. The quantity of the adsorbed reagent at equilibrium (Q_e, in mg.g^{-1}) is calculated by equation (eq-1).

The following four models, in their linear form, are used to describe the adsorption isotherms:

- The Lungmuir model [14]:

$$Q_e = \frac{Q_m K_L C_e}{1+K_L C_e} \quad (eq.3)$$

This equation can be reshaped and rearranged into linear of the following equations [15].

$$\frac{C_e}{Q_e} = \frac{C_e}{Q_m} + \frac{1}{Q_m K_L} \quad (eq.4)$$

Q_e is the amount (mg.g^{-1}) of RR-23 adsorbed at equilibrium; this is the equilibrium concentration (mg.L^{-1}); Q_0: the monolayer adsorption capacity (mg.g^{-1}); K_L: the Lungmuir constant (L.mg^{-1}) related to the adsorption free energy.

An essential characteristic of the Lungmuir isotherm can be expressed in terms of a dimensionless constant called the separation factor and defined by the equation below [16].

$$R_L = \frac{1}{1+K_L C_0} \quad (eq.5)$$

Where C_0 is the initial concentration of the adsorbate (mg.L^{-1}) and K_L is the Lungmuir constant (L.mg^{-1}). A separation factor $R_L > 1$ indicates that the adsorption is unfavorable, if $R_L = 1$ the adsorption is said to be linear, adsorption is said to be favorable when $0 < R_L < 1$, and a zero separation factor ($R_L = 0$) Indicates that adsorption is irreversible. In our case, the found values of R_L are all between 0 and 1, which reveals favorable adsorption.

- The Freundlich equation:

The Freundlich isotherm was used for heterogeneous sorption and to describe the adsorption of organic and inorganic components in the solution [17]. The Freundlich isotherm has a linear expression, as shown by eq.6.

$$Ln\, Q_e = \frac{1}{n} Ln\, C_e + Ln\, K_F \quad (eq.6)$$

K_F is a constant indicating the relative adsorption capacity of the adsorbent (mg.g^{-1}) and 1/n indicates the adsorption intensity. These constants are determined from the equation of the line ($Ln\, Q_e$) = f(LnC_e).

- The Temkin equation [18]:

$$Q_e = \frac{RT}{b} Ln\, C_e + \frac{RT}{b} Ln\, K_T \quad (eq.7)$$

Where T: absolute temperature in °K, R: perfect gas constant (8.314 J.mol^{-1}.K^{-1}), B_1 (J.mol^{-1}): adsorption heat; K_T (L.mg^{-1}): constant corresponding to the maximum equilibrium binding energy.

- The equation of Dubinin-Radushkevich [2]

$$Ln\, Q_e = -K_D\, \varepsilon^2 + Ln\, Q_m \quad (eq.8)$$

□: the potential of Polanyi, corresponding to:

$$\varepsilon = RTLn\left(1 + \frac{1}{C_e}\right) \quad (eq.9)$$

And K_D: the adsorption constant per molecule of the adsorbate when it is transferred to the surface of the solid from the infinite in the solution [19]. K_D and E (KJ.mol^{-1}) are linked by the relationship

$$E = \frac{1}{\sqrt{2K_D}} \quad (eq.10)$$

3. RESULTS AND DISCUSSION

3.1 Effect of various parameters on the elimination of AO-52

3.1.2 Effects of pH on removal of AO-52

The effect of pH on the removal of AO-52 using a BCCLS and the BCCLSh are shown in figure 6.

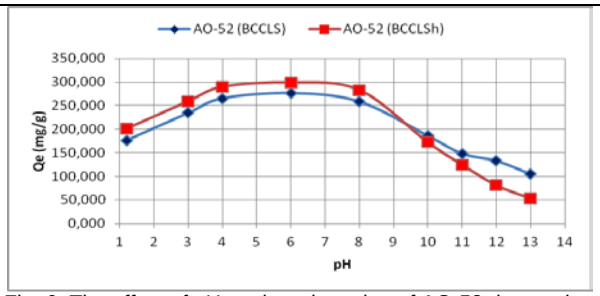

Fig. 6. The effect of pH on the adsorption of AO-52 dye on the BCCLS and BCCLSh. (*t=90 min; T=30±1°C, C_0=300mg.L^{-1}; Adsorbent mass=50mg; Stirring=200 rpm).*

The effect of pH on the adsorbed amount is very important for both adsorbents. At acidic pH the amount adsorbed by BCCLS and BCCLSh varies rapidly from 176.4 to 265.05mg.g^{-1} and from 201.31 to 290mg.g^{-1} as the pH increases from 1.2 to 4, for the two materials respectively. This variation due to the formation of hydrogen bonds at the surface of adsorbents or the number of proton H^+ becomes important; hence there is an increase in the active sites. When the pH increases from 4 to 8 the adsorbed quantity remains almost constant (low variation) so the biochar of the two materials is saturated. At 8 <pH the adsorbed amount rapidly depleted for the BCCLS and BCCLSh, while the amount adsorbed by the BCCLS decreased from 258.07 to 105.23mg.g^{-1} and for the BCCLSh from 283 to 53.23mg.g^{-1}. This important variation can be due to the increase of the HO^- ions which blocks the adsorption by the occupation of the active sites in the adsorbate.

3.1.1 Effects of dose adsorbent on removal of dye.

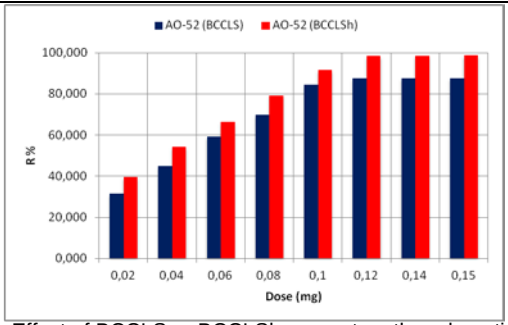

Fig. 7. Effect of BCCLS or BCCLSh amount on the adsorption of AO-52 dye, *(Time = 90 min, Temperature T = 30 ± 1°C, Initial concentration of dye = 300 mg.L^{-1}, Agitation 200rpm and pH = 7 ± 0.5)*

Figure 7 shows the variation in AO-52 dye removal performance by BCCLS and BCCLSh. When the mass varies from 20mg to 120mg the dye elimination efficiency increases from 31.18 to 87.45% for the BCCLS and from 39.3 to 98.34% for the BCCLSh. For the adsorbate mass range from 120mg to 150mg the dye elimination yield varies from 87.45 to 87.53% and from 98.34 to 98.65% for the two materials BCCLS and BCCLSh respectively. It can be concluded that when the mass of adsorbate is greater the elimination of the dye does not evolve, so we will have the balance between the adsorbate and the adsorbent or graduations of the concentration (formation of micro-battery concentration).

3.1.3 Effect of initial concentration on removal of dye

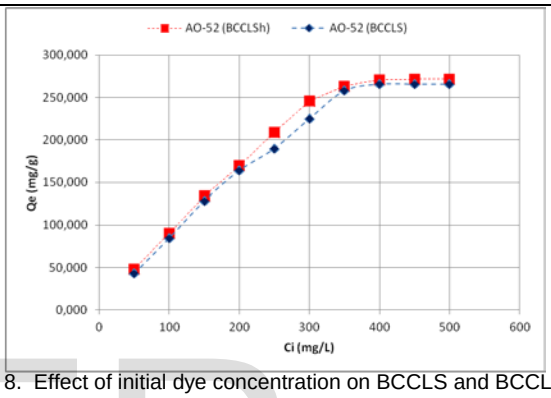

Fig. 8. Effect of initial dye concentration on BCCLS and BCCLSh adsorption (t = 90min, T =30±1°C, Stirring = 200rpm and pH=7±0.5)

The effect of the initial concentration of AO-52 in the range of 50-500 mg.L^{-1} on the percentage removal and absorption of AO-52 dye by BCCLS and BCCLSh were studied under experimental conditions, the results are shown in figure 8. At dye concentrations below 350mg.L^{-1}, the ratio of AO-52 to vacant BCCLS sites or BCCLSh are high, resulting in increased elimination dyes and transfer to the absorbent surface by migration and convection. At higher dye concentrations, the lower percent removal is due to active site saturation for both bioadsorbent, and a possible repellency between the adsorbed layers and the remaining bulk molecules. The data show that AO-52 uptake by the BCCLS increases from 42.88 to 257.63mg.g^{-1} and AO-52 removal percentage decreases from 85.75 to 73.61% with an increase in dye concentration of 50 to 350mg.L^{-1}. On the other hand, for the BCCLSh, the percentage of elimination of AO-52 decreases from 97.08 to 75.23% with the same concentration. For concentrations greater than 350mg.L^{-1} adsorbed amount remains almost constant ranges from 265.46 to 265.55 mg.g^{-1} for the BCCLS and from 271.15 to 271.23 mg.g^{-1} for BCCLSh .In fact, the increase of the concentration induces an increase

in the driving force of the concentration gradient, thus increasing the diffusion of the dye molecules in solution across the surface of the adsorbent.

3.1.4 The effect of contact time

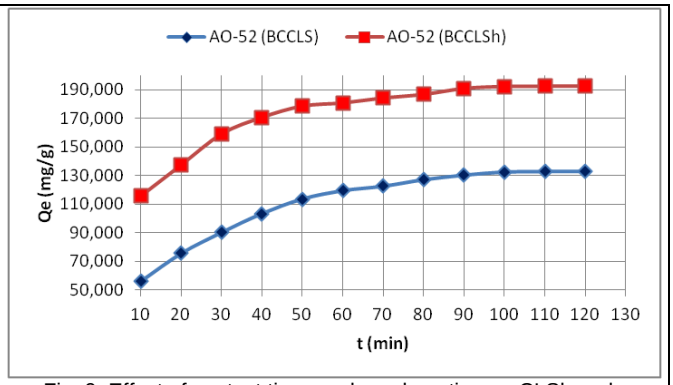

Fig. 9. Effect of contact time on dye adsorption on CLSh and BCCLSh *(T = 30 ± 1°C, C_0 = 300mg.L-1, Stirring=200 rpm and pH =7 ± 0.5)*

The evolution of the adsorbed amount of the AO-52 dye per gram of BCCLS or BCCLSh as a function of the contact time at an initial dye concentration set at 300 mg.L^{-1}, figure 9 shows that the adsorbed quantity varies rapidly from 56.23 to 130.23 mg.g^{-1} for the BCCLS and from 115.92 to 190.77mg.g^{-1} for the BCCLSh when the contact time increases from 10 to 90 min. can infer that the selectivity of the BCCLSh is greater than that of BCCLS. In a ranging time from 90 to 120min the amount adsorbed by the BCCLS goes from 130.23 to 132.92mg.g^{-1} and for the BCCLSh goes from 190.77 to 192.46mg.g^{-1}.

3.2. Adsorption Kinetics

The four models of the kinetics tested are presented in figure 10. The choice of the best model established for the study of the adsorption kinetics is selected as a function of the correlation factor. From the results of figure 10 and table 4, we find that the model with the highest correlation factor is the pseudo-second order model (R^2 = 0.998 for BCCLS and R^2=0.999 for BCCLSh), we can deduce that the pseudo-second order is that which describes the adsorption process of the AO-52 dye on the BCCLS and the BCCLSh, we also see that the adsorbed quantities calculate $Q_{e,cal}$ by this model and The adsorbed experimental quantities $Q_{e,exp}$ are closer.

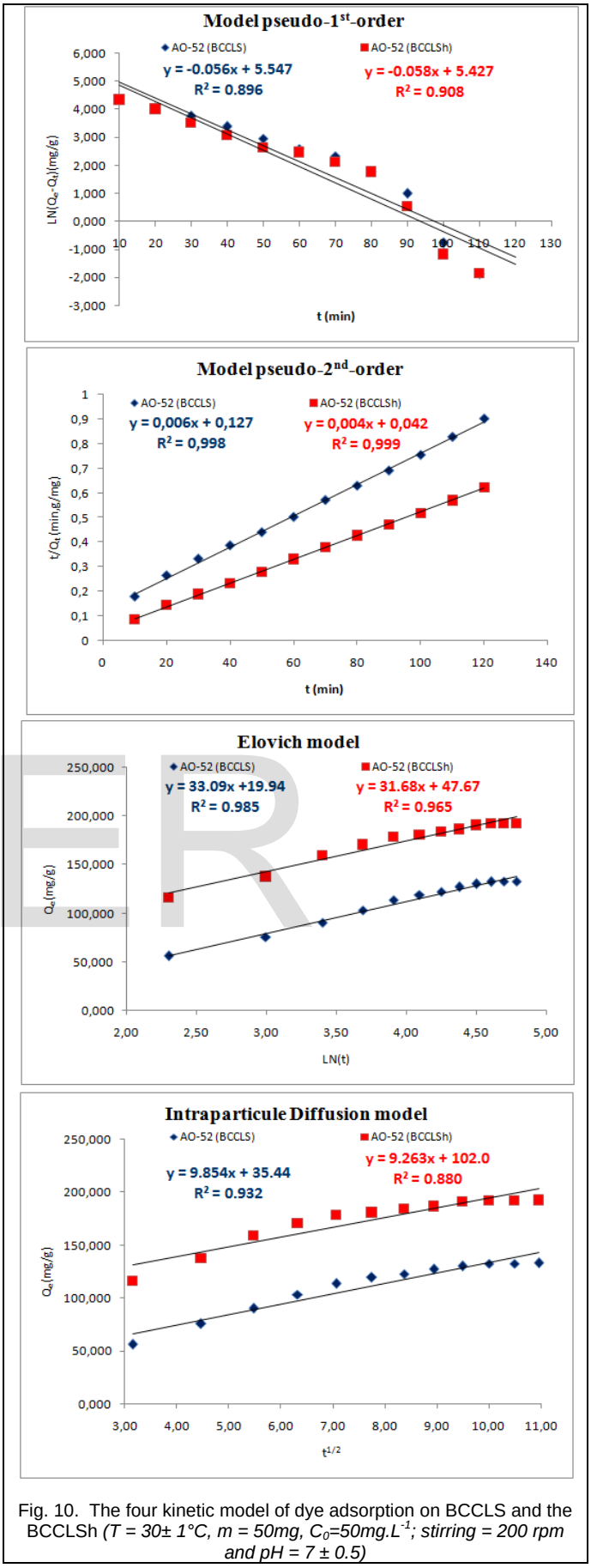

Fig. 10. The four kinetic model of dye adsorption on BCCLS and the BCCLSh *(T = 30± 1°C, m = 50mg, C_0=50mg.L^{-1}; stirring = 200 rpm and pH = 7 ± 0.5)*

TABLE 4

ADSORPTION KINETICS CONSTANTS OF RR-23 ON CLSH AND THE BCCLSH (T= 30 ± 1°C, M =50 MG, C0= 50 MG.L-1; STIRRING = 200 RPM AND PH = 7 ± 0.5)

models	The constants	BCCLS	BCCLSh
Pseudo-1st-order	R^2	0.896	0.908
	K_1(ml.min^{-1})	0.056	0.058
	$Q_{e,cal}$ (mg.g^{-1})	256.47	227.47
	$Q_{e,exp}$ (mg.g^{-1})	130.23	190.77
Pseudo-2nd-order	R^2	0.998	0.999
	K_2(g.mg^{-1}.min^{-1})	0.0028	0.00038
	$Q_{e,cal}$ (mg.g^{-1})	166.67	250
	$Q_{e,exp}$ (mg.g^{-1})	130.23	190.77
Elovich model	R^2	0.985	0.965
	α (mg.g^{-1}.min^{-1})	60.47	142.64
	β (g.mg^{-1})	0.0302	0.03156
Intraparticule diffusion model	R^2	0.932	0.880
	K_i (mg.g^{-1}.min$^{0.5}$	9.854	9.263
	C (mg.g^{-1})	35.44	102

R^2: coefficient of determination; Q_e: amount of RR-23 adsorbed at equilibrium; K_1: First-order adsorption rate constant; K_2: velocity constant of the second order of adsorption α: initial rate of adsorption; β: desorption constant; K_i is the intraparticule diffusion constant. C: The value of the intercept.

3.3Adsorption isotherms

The adsorption isotherm indicates how the molecules are distributed between the liquid phase and the solid phase when the adsorption reaches equilibrium. In this study, the isotherms models studied are the Langmuir model, Freundlich model, Temkin model and the Dubinin-Radushkevich model .The most frequently established model for the study of adsorption isotherms is chosen as a function of the correlation factor. The model of Langmuir is the model applied in the adsorption of AO-52 for the two materials, which is a correlation factor (R^2 = 0.988) for the BCCLS and (R^2=0.993) for the BCCLSh. The maximum adsorbed amount by the BCCLS and BCCLSh are equal to 333.333mg.g^{-1} and 500 mg.g^{-1} respectively. The isothermal constants obtained by linearization of the various models considered are summarized in table 5, while the correlation between the experimental values and those predicted by the best model is illustrated in figure 11.

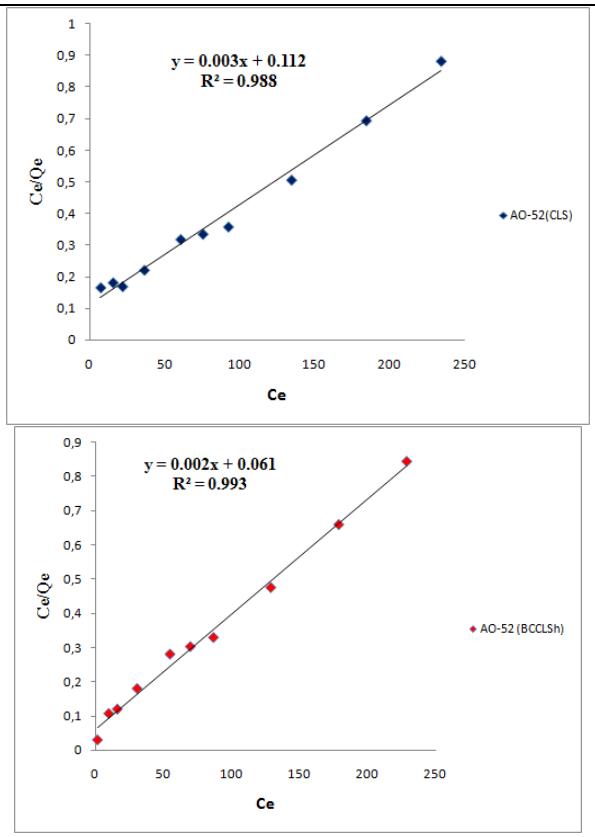

Fig.11. The Lungmuir Isotherms for the adsorption of AO-52 on the BCCLS and BCCLSh *(T=30±1°C, m= 50 mg, stirring = 200 rpm and pH =7± 0.5)*

TABLE 5

CONSTANT ADSORPTION ISOTHERMS OF AO-52 ON BCCLS AND BCCLSH (T = 30 ±1° C, M = 50 MG, AGITATION = 200 RPM AND PH = 7 ± 0.5)

Models	Constants	BCCLS	BCCLSh
Lungmuir Isotherm	R^2	0.988	0.993
	R_L	0.0694 - 0.4273	0.0132 - 0.1182
	K_L (*L.mg^{-1}*)	0.0268	0.1492
	Q_m (*mg.g^{-1}*)	333.333	500
Freundlich Isotherm	R^2	0.899	0.965
	K_F	21.867	44.523
	n	1.972	2.739
Temkin Isotherm	R^2	0.96	0.942
	K_T (*L.g^{-1}*)	0	1,0896
	B_1 (*J.mol^{-1}*)	70.61	51.32
	b	35.677	49.087
Dubinin-Radushkevich Isotherm	R^2	0.811	0.631
	K_{ad} (*mol^2.Kj^{-2})*10^{-5}*	2	0.09
	E(*Kj.mol^{-1}*)	158.114	745.356
	Q_m (*mg.g^{-1}*)	213.151	201.140

Various studies on the removal of methyl orange or orange acid (AO-52) by different biomass or composite

from wastewater are shown in Table 6 to show the optimum dye removal conditions and maximum adsorption quantities.

TABLE 6

ADSORPTION CAPACITY AND EXPERIMENTAL CONDITIONS OF DIFFERENT BIOMASSES OR COMPOSITE FOR THE REMOVAL OF METHYL ORANGE DYE IN WASTEWATER.

Adsorbent	Mesoporous TiO_2	Multiwalled Carbon Nanotubes	Mg – Al Layered Double Hydroxide	Calcined Lapindo Volcanic Mud	Mesoporous Carbon	Chitosan/Maghemite Composite	Multiwalled Carbon Nanotubes	Activated Carbon Derived From Phragmites Australis	Zinc Oxide Loaded Activated Carbon (ZnO-AC)
R^2	0.995	***	0.993	0.999	0.866	0.990	0.990	0.988	0.988
Isotherm Model	Freundlich	****	Langmuir	Langmuir	Langmuir	Langmuir	Langmuir	Timken	Langmuir
R^2	--	0.95	--	0.999	0.999	0.98	0.998	1	0.999
Kinetic isotherm	Pseudo-2nd order	Pseudo-2nd order	Pseudo-2nd order	Pseudo-2nd order	Pseudo-2nd order	Pseudo-2nd order	Pseudo-2nd order	Pseudo-2nd order	Pseudo-2nd order
Temps (min)	20	140	120	120	60	300	120	240	120
T(°C)	80	20	25	30	25	20	25	30	40
pH	5	***	6.5	3	3.3	4.1	7	4	7
C_0(mg/L)	100	200	300	100	1000	70	20	50	50
Q_m(mg/g)	454.5	52.2	151.12	333.33	249.1	779	51.74	127.39	153.8
Ref	[20]	[21]	[22]	[23]	[24]	[25]	[26]	[27]	[28]

From the results of Table 6 it can be seen that the elimination of AC-52 by the different biomass presents a quantity of adsorption less than that found in our study which is equal to 500 $mg.g^{-1}$ for BCCLSh and 333.33 $mg.g^{-1}$ for BCCLS

Conclusion

The present work has clearly established the utility of pyrolysis-synthesized biochar in the optimum condition that will be used in adsorption of AO-52 one dye. The experiments show a considerably increasing its adsorption properties for the removal of orange acid 52 in the industrial waters. The observed that the removal content AO-52 increased with increasing pH (up to the optimum), the temperature, the adsorbent and the adsorbate concentration. In the same time, the maximum removal yield of AO-52 by the BCCLS and BCCLSh was carried out for the initial concentration of 300 $mg.L^{-1}$, temperature of 30°C and pH 7±0.5. The adsorption kinetics study follow the pseudo-second-order model with adsorption quantity equal to 250$mg.g^{-1}$ for the BCCLSh and 166.67$mg.g^{-1}$ for the BCCLS, as well as the Langmuir model, is the most applicable in the adsorption isotherm with an adsorption quantity of 500$mg.g^{-1}$ for the BCCLSh and 333.333$mg.g^{-1}$ for the BCCLS.

References

1. Hwang, M. C. and Chen, K. M., "Removal of color from effluents using polyamide–epichlorohydrin-cellulose polymer. II. Use in acid dye removal", *J. Appl. Polym. Sci*. 49(6), (1993): 975–989.
2. El Farisssi, H., Lakhmiri, R., Albourine, A. Safi, M., Cherkaou,O "Removal of RR-23 dye from industrial textile wastewater by adsorption on cistus ladaniferus seeds and their biochar", *J. Environ. Earth Sci.* 7(11): (2017). 105–118
3. El Fargani, H., Lakhmiri, R., Albourine, A. Safi, M., "Modified Chitosan Immobilized on Modified Sand for Industrial Wastewater Treatment in Multicomponent Sorption : Shrimp Biowaste Processing". *Chemistry and Materials Research*. **9**(4) (2017): 20–42
4. Mohammad, N., Salehi, R., Arami, M., Bahrami, H., "Dye removal from colored textile wastewater using chitosan in binary systems," *DES*, 267(1), (2011): 64–72
5. El Fargani, H., Lakhmiri, R., El Farissi, H., Albourine, A., Safi, M., Cherkaoui, O., "Removal of anionic dyes by silica-chitosan composite in single and binary systems : Valorization of shrimp co- product „ Crangon - Crangon " and „ Pandalus Borealis , *JMES*, **8**(2), (2017): 724–739,
6. El Farissi, H., Lakhmiri, R., El Farissi, H., Albourine, A., Safi, M., "Valorisation of a Forest Waste (Cistus Seeds) for the Production of Bio-Oils," *JMES*, **8**(2), (2017): 628–635.
7. El Farissi, H., Lakhmiri, R., Albourine, A., Safi, M., "Production of Bio-Oil from Cistus Ladanifer Shell by Fixed-Bed Pyrolysis," *IJENS-IJET*, 17(4), (2017): 25-30
8. Lagergren S., Hand., 24, (1898): 1–39

9. HO, Y. S "Citation review of Lagergren kinetic rate equation on adsorption reactions," *Scientometrics,* 59 (1), (2004): 171–177
10. Ho, Y. S., McKay, G., "Pseudo - second order model for sorption processes", *Process Biochemistry* 34, (1999): 451- 465,
11. Ho, Y. S., Mckay, G., "Sorption of dyes and copper ions onto biosorbents," *Process Biochem*. 38, (2003): 1047-1061
12. Chien,S.H., Clayton,W.R., " Application of Elovich equation to the kinetics of phosphate release and sorption in soils", *Soil Sci. Soc. Am. J .,* 44 , (1980): 265-268
13. Urano. K., and Hirotaka. T., "Process Development for Removal and Recovery of Phosphorus from Wastewater by a New Adsorbent. 2. Adsorption Rates and Breakthrough Curves‟ *Ind. Eng. Chem. Res.* 30, (1991): 1897-189
14. Langmuir. I., *Am. J., Chem. Soc.*, 40, (1918): 1361–1403
15. Ghasemi. M., Javadian. H., Ghasemi. N., Agarwal. S., Gupta. V.K., *Journal of Molecular Liquids,* 215, (2016): 161–169
16. Sujoy, K. D., Jayati, B., Akhil, R. D., "Adsorption Behavior of Rhodamine B on Rhizopus o ryzae Biomass," *Langmuir,* 22(17), (2006): 7265–7272
17. Laabd, M., Chafai, H., Essekri, A., Elamine, M., Lakhmiri, R., and Albourine A., "Single and multi-component adsorption of aromatic acids using an eco-friendly polyaniline-based biocomposite," *Sustain. Mater. Technol.* (2017)
18. Ghasemi. M., Javadian. H., Ghasemi. N., Agarwal. S., and Gupta. V.K., Journal of Molecular Liquids, 215, (2016): 161-169
19. William, J., Weber, Navrotsky, A., Stefanovsky, S., "Materials Science of High-Level Nuclear Waste Immobilization." 34 (1), (2011): 46-53
20. Asuha S., Zhou X. G., and Zhao S., "Adsorption of methyl orange and Cr(VI) on mesoporous TiO2 prepared by hydrothermal method," *J. Hazard. Mater.,* 181, (1–3), (2010): 204–210,
21. Zhao D., Zhang W., Chen C., and Wang X., "Adsorption of Methyl Orange Dye Onto Multiwalled Carbon Nanotubes," *Procedia Environ. Sci.*, 18, (2013): 890–895,
22. Ai L., Zhang C., and Meng L., "Adsorption of Methyl Orange from Aqueous Solution on Hydrothermal Synthesized Mg - Al Layered Double Hydroxide," *J. Chem. Eng. Data,* 56, (2011): 4217–4225,
23. Jalil A., "Adsorption of methyl orange from aqueous solution onto calcined Lapindo volcanic mud," *J. Hazard. Mater*., 181, (1–3), (2010): 755–762
24. Mohammadi N., Khani H., Gupta V. K., Amereh E., and Agarwal S., "Adsorption process of methyl orange dye onto mesoporous carbon material-kinetic and thermodynamic studies," *J. Colloid Interface Sci*., 362 (2), (2011): 457–462.
25. Obeid L., "Chitosan/maghemite composite: A magsorbent for the adsorption of methyl orange," *J. Colloid Interface Sci.,* 410, (2013): 52–58,
26. Yao Y., Bing H., Feifei X., and Xiaofeng C., "Equilibrium and kinetic studies of methyl orange adsorption on multiwalled carbon nanotubes," *Chem. Eng. J.,* 170(1), (2011): 82–89,
27. Chen S., Zhang J., Zhang C., Yue Q., Li Y., and Li C., "Equilibrium and kinetic studies of methyl orange and methyl violet adsorption on activated carbon derived from Phragmites australis," *Desalination,* 252(1–3), (2010):149–156,
28. Saini J., Garg V. K., Gupta R. K., and Kataria N., "Removal of Orange G and Rhodamine B dyes from aqueous system using hydrothermally synthesized zinc oxide loaded activated carbon (ZnO-AC)," *J. Environ. Chem. Eng*., 5(1), (2017): 884–892.